# Visualizing and Quantifying Interactions in the Excited State.

Laurent Vannay[†], Eric Bremond[†‡], Piotr de Silva[†§] and Clémence Corminboeuf[†,*]

[†]Laboratory for Computational Molecular Design, Ecole Polytechnique Fédérale de Lausanne, CH-1015 Lausanne, Switzerland

[‡]CompuNet, Istituto Italiano di Tecnologia, via Morego 30, I-16163 Genoa, Italy.

[§]Department of Chemistry, Massachusetts Institute of Technology, Cambridge, Massachusetts 02139, USA

Address correspondence to: clemence.corminboeuf@epfl.ch (CC)

## ABSTRACT

**Determining the location and nature of the electron pairs within a molecule provides an intuitive representation of electronic structures. Yet, most of the available theoretical representations are not suitable for describing excited state phenomena. The Density Overlap Region Indicator (DORI) scalar field, which depends only on the density and its derivatives, overcomes previous limitations, while keeping the intuitiveness of popular scalar fields. We here demonstrate its usefulness by pinpointing visual and numerical DORI signatures for both intra- and intermolecular excited state situations.**

## Introduction

The analysis of covalent bonding patterns and intermolecular interactions via electronic structure methods has helped rationalizing a myriad of chemical phenomena. Within this context, the direct analysis of the wavefunction that is an eigenstate of an electronic Hamiltonian provides the complete information about the corresponding stationary state; and thus of the electronic structure of the system (in this particular state). Unfortunately, the wavefunction is an extremely complex object, which depends on the positions and spins of all the electrons; therefore analyzing details or comparing many-electron wavefunctions is virtually impossible owing to various practical difficulties. To remedy this inconvenience, much effort has been put into connecting electronic structure theory with classical chemical concepts, of which chemical bonding is the most prominent example. The most fundamental approach is to analyze molecular orbitals, a set of one-particle wavefunctions, which appear in most of the electronic structure methods. Another strategy is to condense the relevant information into a single three-dimensional function of space – a molecular scalar field. The common rationale for constructing such fields is to define a measure of electron localization,[1–4] which links the results of computations to concepts like bonds, electron cores and lone pairs. Such descriptors are based on some local representation of the kinetic energy, which is typically computed from molecular orbitals. While these functions have become very insightful for probing the structure of ground states, similar analysis of bonding in the excited state is a field relatively unexplored except for the lowest triplet or quintet states[5–8] of single organic molecules and coordination compounds (*i.e.,* ground state computations enforcing triplet or quintet spin state) and for the analysis of benzene and naphthalene excimers[9] using the non-covalent interaction index (NCI)[10] or alternative real-space partitioning (e.g., quantum theory of atoms in molecules QTAIM[11,12] or the Parity Function[13]) that are somewhat more cumbersome to interpret.[14–17] The analysis of excited states using localization functions is limited by the dependences on molecular orbital, which are not well defined in the excited state. Most popular descriptors like the electron localization function (ELF)[1] and localized orbital locator (LOL)[3] also makes a reference to the homogenous electron gas (HEG) model to achieve a dimensionless quantity. These dependencies render the extension beyond ground state situations non-trivial.[18] More recently, methods capable of simulating orbitals in the excited state have been proposed[19,20] but they are not yet extensively available. 3D or 2D representation of alternative functions that rely on the electron density and its derivatives and are thus orbital-free have also been proposed[10,21–26] but they yet have to be applied to the excited states, as emphasized in this work.

Even if the application of localization functions to excited states was straightforward, the comparison of the ground and excited-state pictures of localization functions would not necessarily help characterizing the nature of an electronic transition. In particular, it would not reveal much information about the changes occurring in regions where the electrons are not well localized (e.g., Rydberg or excimeric states). Often, the relevant question to ask about the excited state is not where are the electrons localized, but rather where have they moved to upon excitation. Answering this question enables to determine the character of the excited state; thus distinguish between e.g. local, Rydberg or charge transfer excitations. Akin to the ground state's analysis, it is a common practice to look at the occupied and virtual canonical orbitals involved in the excitation but such analysis is very much basis set dependent.[27] A set of powerful methods for analysis of electronic transitions is based on diagonalization of transition and difference density matrices. The examples are natural transition orbitals,[28–30] and the so-called attachment/detachment densities[31] (see Refs [32][33] for an excellent review). Insights into the excited state characters can also be retrieved from excitation localization distribution,[34,35] transition dipole moments and more scarcely from computations in the framework of conceptual density functional theory (e.g. state-specific dual descriptor).[36]

As outlined above, the majority of localization descriptors and electronic transition analysis methods relies in practice on the one-electron basis, either directly through orbitals or one-particle density matrices. This is a very convenient representation, as it can directly relate to the particle-hole picture of an excitation. Nevertheless, it is tantalizing to ask what can be learned about an excited state solely from its electron density. This appears to be a much more challenging task as the density itself is rather featureless; its direct analysis does not bring much information about the character of the transition as all the relevant densities look very similar. One possible way of extracting information is to look at density difference, which requires only densities of the excited and ground states. Density difference gives information about the character of the transition, but provides no insight into the bonding and interactions in the excited state.

Here, we make a first attempt to unify the description of interatomic and intermolecular interactions with the elucidation of the transition's character by analysis of the geometric features of the electron density. To this end, we employ the Density Overlap Region Indicator (DORI),[26] a bonding descriptor recently proposed by two of us. DORI is a dimensionless scalar field that depends solely on the electron density, $\rho(\mathbf{r})$, and its derivatives:

$$\mathrm{DORI}[\rho(\boldsymbol{r})] = \frac{\theta[\rho(\boldsymbol{r})]}{1 + \theta[\rho(\boldsymbol{r})]} \qquad (1)$$

where

$$\theta[\rho(\boldsymbol{r})] = \frac{\left(\nabla\left(\frac{\nabla\rho(\boldsymbol{r})}{\rho(\boldsymbol{r})}\right)^2\right)^2}{\left(\frac{\nabla\rho(\boldsymbol{r})}{\rho(\boldsymbol{r})}\right)^6} \qquad (2)$$

Its values in the [0,1] range make it straightforward to use as well as system independent. Since DORI (**r**) = 0 for the hydrogen atom and DORI (**r**) = 1 for the uniform electron gas, the values of DORI can be interpreted as a measure of the density inhomogeneity on a range going between these two paradigm densities. Its ability to reveal regions of clash between molecular, atomic or shell densities (see Figure **1**) stems from the fact that the density tails of of finite systems decay exponentially (hydrogen-like). The overlap of two finite systems (even non-interacting) perturbs the density, which then deviates from the single-exponential behavior and becomes more uniform. Hence, DORI discovers both covalent bonding patterns and non-covalent interactions and is thus very convenient to analyse both ground and excited state phenomena. Recent examples of DORI applications can be found in Refs[37,38]. It is also worth mentioning that DORI has been successfully used as an ingredient of semi-local and local hybrid exchange-correlation functionals.[39,40]

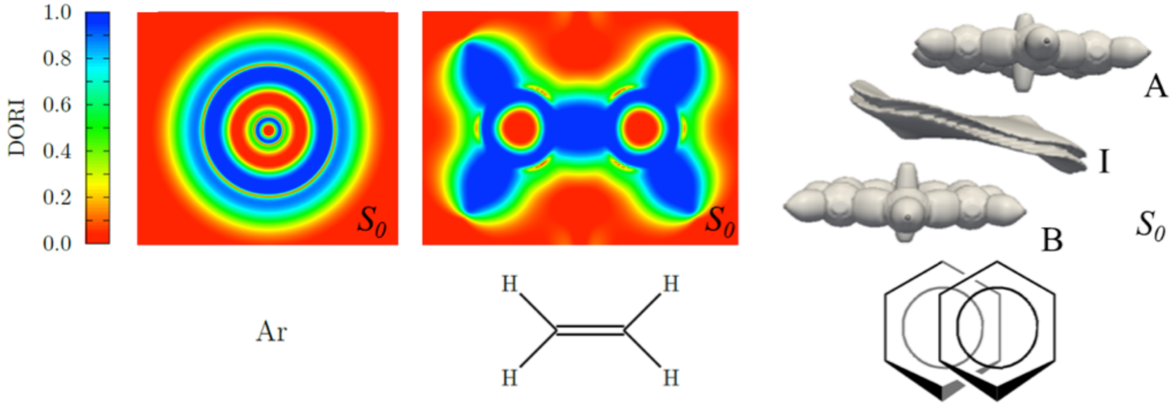

**Figure 1**: Two-dimensional ground state DORI maps of the argon atom (left) and in the $\sigma_h$ plane of the ethene molecule (middle). Three dimensional representation of the ground state DORI for the parallel-displaced benzene dimer (right) plotted for DORI[□$_{s0}$] = 0.95. DORI computations uses a density self-consistently optimized at the B3LYP[41]/TZP level.

Here, we anticipate that differences in density overlaps will carry information about the character of the excited state, either by appearance of new overlap regions or detectable changes in those present already in the ground state. More specifically, we use DORI to visualize and quantify the electronic and geometric changes affecting molecular systems upon electronic excitations. For this purpose, we selected prototypical molecules and complexes that exhibit clear excited state signatures (e.g., Rydberg, $\pi$ –$\pi$*, excimer, charge transfer). These examples include pyrrole, aromatic chameleons[42], excimers formed by (poly-)aromatic hydrocarbons, donor-acceptor complexes and an iridium dye. The excited state densities are retrieved from a Time-Dependent Density Functional Theory (TDDFT)[43] computations (see computational details). Note that the forthcoming discussion focuses on the use of DORI to characterize the nature of electronic excitation and not on the problematic energy ordering of these excitations within TDDFT (e.g., Rydberg and charge transfer states). Still, we verified that the density-based trends that are presented herein are valid regardless of these shortcomings. We also insist that a density-based descriptor like DORI does not rely on any one-particle basis and is thus applicable at any level of theory or even experimental densities. It is compatible with any density computed from wavefunction-theory based methods (e.g., CASSCF, CC), orbital-free approaches or computations that do not use atom-centered basis sets (e.g., plane-waves, grids).

## COMPUTATIONAL Details

Monomers were optimized in their ground states at the $\omega$B97X-D/def2-SVP level[44,45] in Gaussian'09[46] except for the polyaromatic hydrocarbons, which were optimized in the ADF2013.01 code[47–49] at the B3LYP/TZP level.[41,50] Excimer geometries were obtained through optimizing the first excited singlet state at the $\omega$B97X-D/def2-SVP level starting from a parallel arrangement of the two monomers at 3.2 Å. The charge transfer complexes and the iridium dye were optimized at the ωB97X-D/def2-SVP level. The LANL2DZ basis set was used to describe the iridium atom. All the ground state DFT densities were self-consistently optimized with standard convergence criteria by a Kohn-Sham procedure as implemented in ADF2013 and Gaussian'09. With each software, excited-state densities were obtained by adding to the converged DFT wavefunction the necessary Z-vector contribution derived from a coupled-perturbed Kohn-Sham (CPKS) calculation to produce the relaxed density for state $N$.[51] [52] The $\mathrm{DORI}_{\mathrm{int}}$ values were computed by a numerical integration of the density within a DORI basin using a 0.1au mesh grid with a locally modified version of DGRID[53] available on demand. The Paraview software[54] was used to get a visual representation of the DORI function. Alternatively, DORI is now available for ground states in ADF2016.[55]

## RESULTS AND DISCUSSION

### Molecular Excitations

Rydberg excitations provide the first illustrative class of patterns elegantly captured by DORI. Taking pyrrole as a prototypical example,[e.g., 54–57] we show that those diffuse excitations are easily recognizable by the formation of a characteristic DORI basin located around the molecule (Figure 2). This density clash originates from the overlap between the newly populated Rydberg region and the valence electrons. At the chosen TD-PBE0[60] /TZVP-aug level (see Ref. [59] for additional discussion), the first three excited state singlets of pyrrole have a Rydberg signature (see Figures S1 in the SI for molecular orbitals and density differences). The clash of the first excited state $S_1$ ($1A_2$) ((HOMO (π)→LUMO (3s)) is essentially localized around the nitrogen atom. The DORI picture after excitation to $S_2$ ($1B_1$) or $S_3$ ($2A_2$) reveals a dominant Rydberg $3p_y$ and $3p_z$ character respectively in line with the molecular orbital picture. Besides the typical Rydberg domains, DORI is also capable of probing the pyrrole covalent bonding regions that remain basically unchanged upon excitation.

Along with the visual signature, a more quantitative analysis can be achieved through integrating the electron density, $\rho(\mathbf{r})$, within the molecular or Rydberg regions defined by a DORI isosurface $V_{\mathrm{iso}}$ such as:

$$\mathrm{DORI}_{\mathrm{int}}\left[\rho_{S_n}, V_{iso}\right] = \int_{V_{iso}} \rho_{S_n}(\boldsymbol{r})\, dr \qquad (3)$$

Upon excitation to a Rydberg state, $\mathrm{DORI}_{\mathrm{int}}$ is compatible with a loss of electrons in the molecular basin (A) (within an isosurface) in favor of the Rydberg basin(s) (Ry). While the obtained numbers obviously depend on the chosen isovalue, the trend for different excited states at the same isovalue reflects the change in density rearrangement as compared to the ground-state.

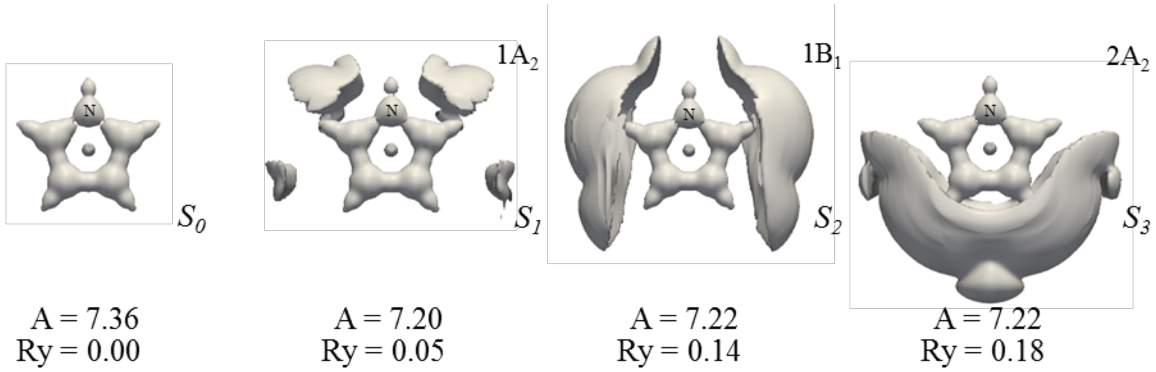

**Figure 2**: DORI=0.85 isosurface and $\mathrm{DORI}_{\mathrm{int}}(\boldsymbol{\rho}_{\boldsymbol{S_n}}, V_{0.85})$, $n \in \{0,1,2,3\}$, for the pyrrole in its ground and the first three (Rydberg) excited state singlets computed at the (TD)-PBE0/TZVP-aug level on the ωB97X-D/def2-SVP ground state optimized geometries. The nitrogen atom position is indicated by "N", $\mathrm{DORI}_{\mathrm{int}}$ for molecular (A) and Rydberg (Ry) basins are given in the Figure.

The electronic structure of the ground ($S_0$) and first π-π* singlet ($S_1$) excited states of biphenylene is a related study case with more pronounced visual changes. As clear from Figure 3, the ground state of biphenylene closely resembles two isolated benzene rings with equalized bond length connected by two single bonds. The DORI isocontour map reveals an imperfect conjugation, which arises from a compromise between maximizing the conjugation behaviour in the 6-membered ring and diminishing the antiaromatic behaviour in the central cyclobutadiene. In sharp contrast, the adiabatic excitation to the first singlet π-π* state leads to a Baird-aromatic 12π electron ring, illustrated by the equalized carbon-carbon bond DORI domains in the periphery. This result is line with Baird's rules[61] and previous experimental and computational studies[62] (see also the exhaustive review[42]) which ascribe an aromatic character to excited state biphenylene and related molecules.[63–66] The structural rearrangement is pronounced but the pure electronic effects visible upon vertical excitation are non-negligible, especially in the region of large π density (see Figure S2). The biphenylene example convincingly shows that information on the bonding patterns in the excited state can be obtained solely from the electron density.

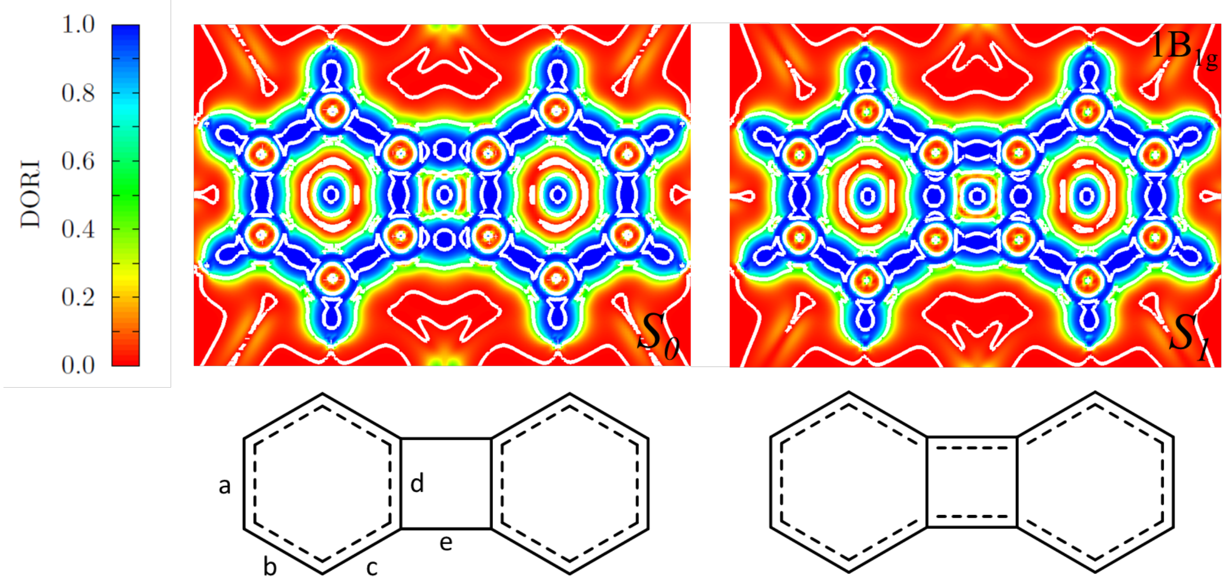

**Figure 3**: Two dimensional ground (top-left) and excited (top right) state DORI maps in the $\sigma_h$ plane of the biphenylene molecule. Isocontour lines of DORI[□]∈{0.01, 0.50, 0.99} are plotted in white. All the structures are optimized at the (TD-)B3LYP/TZP level and the relaxed densities to compute DORI are obtained at the same level. Bottom left and bottom right Lewis structures represent the two schematic electronic delocalization estimated according to the bond length patterns in the ground and excited state, respectively. Bond lengths for ground (excited) state (in [Å]): a=1.38 (1.43), b=1.42 (1.38), c=1.37 (1.40), d=1.42 (1.49), e=1.51 (1.41).

## Excited state complexes

The formation of excimers and exciplexes are alternative typical examples of excited state phenomena occurring between molecules. These excited state complexes that are more strongly bound than their van der Waals ground state minima, possess characteristic lifetimes and light emission properties.[67,68] The binding energy is nevertheless rather weak, on the order of 5-20 kcal mol$^{-1}$ in polyaromatic hydrocarbons (PAHs), and strongly depends upon the geometrical arrangement of the two involved monomers.[69–76] DORI is exploited to provide a characteristic fingerprint for excimers' formation and to identify the nature of the interactions between molecules. Hence, the focus is on the intermolecular DORI domain, where the excimer interaction does occur. Figure 4 displays color-coded DORI taken in the plane parallel to the intermolecular domain of the anthracene dimer.

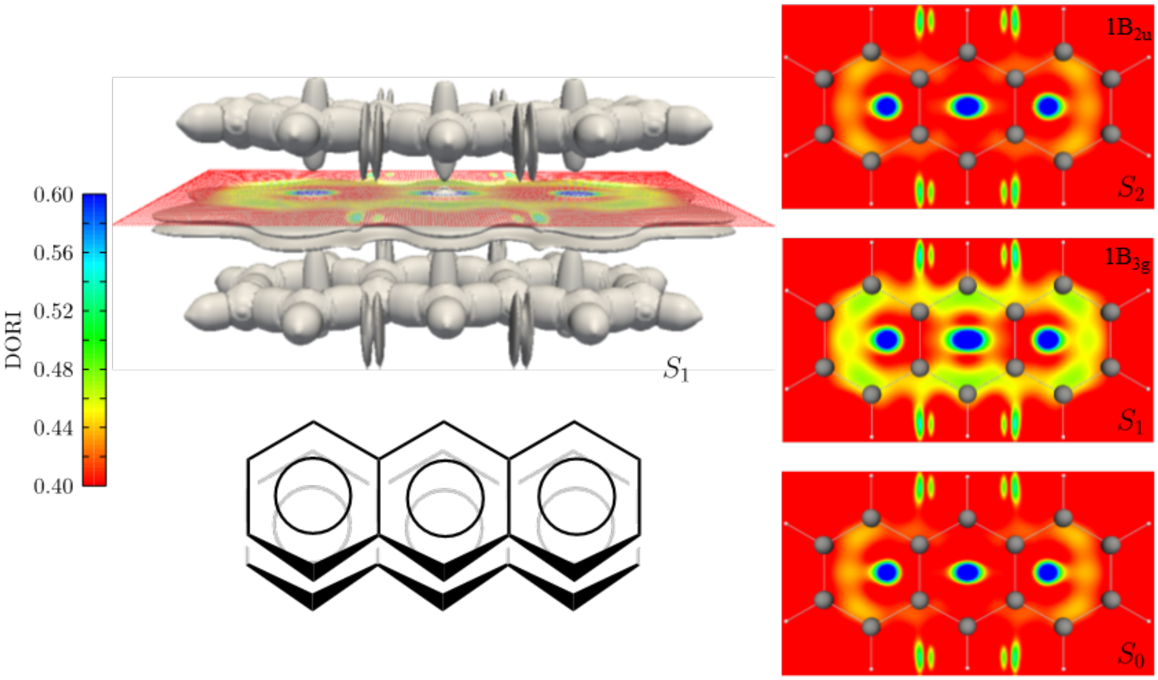

**Figure 4**: (left) Three dimensional representation of the excited state DORI for an anthracene excimer plotted for DORI[$\rho_{s1}$] = 0.7. (right) Two-dimensional ground and excited state DORI maps obtained from relaxed $S_0$, $S_1(1B_{2u})$ and $S_2$ $(1B_{2g})$ (TD-)PBE0/TZP densities. The excimer geometry is optimized at the TD-ωB97X-D/def2-SVP level.

In order to decouple the geometrical and electronic effects, the optimized geometry of the excimer was kept frozen in the $S_1$ (*i.e.*, first excimeric) state and the DORI maps plotted for the $S_0$, $S_1$ (HOMO-LUMO, at the TD-PBE0/TZP level,[60] see Figure S5 for the orbital pictures) and $S_2$ (mixed excitation HOMO-1 → LUMO and HOMO → LUMO) electronic states of the anthracene dimer.

The $S_1$ state has a typical DORI signature, arising from the clearly visible density overlap increase in the intermolecular region. The enhanced π-density overlap is especially apparent above the carbon perimeter (green region, Figure 4) with little participation from the two central bonds. The same pattern characterizes the excimeric states of other PAHs such as pyrene, perylene or benzene (see Figure 5). In contrast, the DORI maps for the ground and non-excimeric $S_2$ excited states of anthracene show a much weaker density overlap. The insights provided by DORI are in line with that of the electron density difference shown in Figure 6 but somehow easier to interpret. Note that the stronger transannular interactions in the excimeric states identified herein, were not captured in the QTAIM and NCI analysis mentioned earlier.[9]

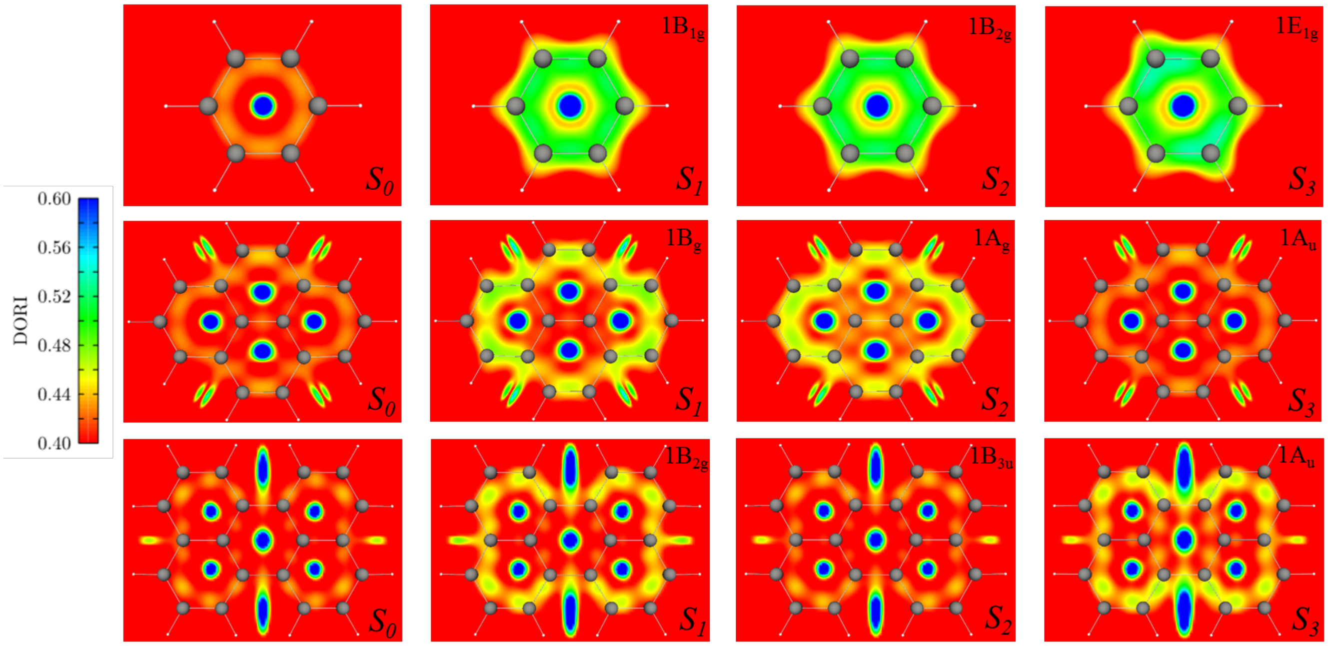

**Figure 5**: DORI maps in the intermolecular plane for the benzene (top), pyrene (middle) and perylene (bottom) dimers using the (TD-)PBE0/TZP densities computed on the $S_1$ excimer ωB97X-D/def2-SVP optimized geometry.

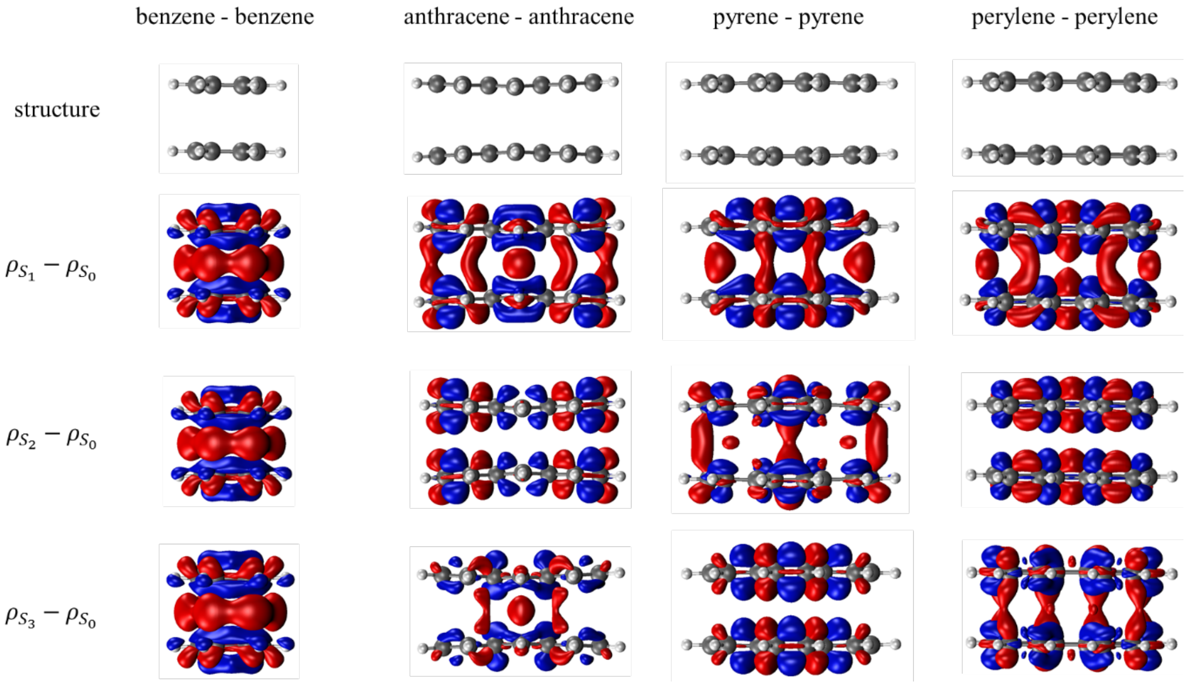

**Figure 6**: Density differences ($\rho_{S_n} - \rho_{S_0}$ , n∈{1, 2, 3}) at the PBE0/cc-pVDZ level[60] for the excimer complexes in their first singlet excited state TD-ωB97X-D/def2-SVP optimized geometry. Isodensities = +0.0005 (red) and -0.0005 (blue).

The integral values within the intermolecular domain have already served to compare the DORI-based electronic compactness in quatertiophene crystals.[26] In the present case, we compare the $\mathrm{DORI}_{\mathrm{int}}$ within three domains, the individual molecules and the intermolecular regions (see **A**, **B** and **I** in Figure 1), in the ground and excited states. The integral variations between the two states can be readily interpreted as a change in the electron number in each region (within a isosurface). As clear from Table 1, all the excimeric states are characterized by a significant loss of electron in the monomers and an increase in the intermolecular region when compared to the ground state. This trend, which is of purely electronic origin, is reflective of the formation and even the magnitude of a bonding region between the dimers. From the integral values, it can also be deduced that the three lowest singlet excited states of the benzene dimer are excimeric with a stronger interaction between the two monomers (large integral values), while negligible integral values (<0.5) are found in the intermolecular domain (**I**) of the local excitations of other complexes (e.g., $S_2$ and $S_3$ in pyrene-pyrene and anthracene-anthracene). These variations are also visible in the DORI maps (see Figure 5).

**Table 1**: $\Delta\mathrm{DORI}_{\mathrm{int}} = [\mathrm{DORI}_{\mathrm{int}}(\boldsymbol{\rho}_{S_n}; V_{0.85}) - \mathrm{DORI}_{\mathrm{int}}(\boldsymbol{\rho}_{S_0}; V_{0.85})]*1000$ in milielectron (me) are computed for atomic (A,B) and intermolecular (I) basins for a series of excimers and charge-transfer complexes using relaxed (TD-)PBE0/cc-pVDZ and (TD-)CAM-B3LYP/cc-pVDZ densities respectively. All charge transfer ground state structures and excimer first excited state structure were optimized at the (TD-)ωB97X-D/def2-SVP level.[44] The geometries of the first excimeric states optimized at the TD-ωB97X-D/def2-SVP level are used for the excimers.

| | $S_1$ | | | $S_2$ | | | $S_3$ | | |
|---|---|---|---|---|---|---|---|---|---|
| systems | A | I | B | A | I | B | A | I | B |
| benzene$_{(A)}$ - benzene$_{(B)}$$^1$ | -37.5 | 37.3 | -37.5 | -46.9 | 39.6 | -46.9 | -43.2 | 40.4 | -43.2 |
| anthracene$_{(A)}$ - anthracene$_{(B)}$$^1$ | -40.5 | 28.2 | -40.5 | -12.1 | 4.5 | -12.1 | -36.3 | 28.6 | -36.3 |
| pyrene$_{(A)}$ - pyrene$_{(B)}$$^1$ | -53.5 | 19.8 | -53.5 | -41.8 | 25.6 | -41.8 | -13.4 | 1.0 | -13.4 |
| perylene$_{(A)}$ - perylene$_{(B)}$$^1$ | -29.4 | 22.7 | -29.4 | -4.6 | 4.0 | -4.6 | -43.0 | 31.9 | -43.0 |
| benzene$_{(A)}$ - TCNE$_{(B)}$$^2$ | -191.6 | -49.8 | 62.8 | -164.8 | -52.7 | 58.8 | 1.7 | -15.4 | -57.9 |
| naphthalene$_{(A)}$ - TCNE$_{(B)}$$^2$ | -152.1 | -26.5 | 57.4 | -160.0 | -25.4 | 60.5 | -147.7 | -19.1 | 53.2 |
| anthracene$_{(A)}$ - TCNE$_{(B)}$$^2$ | -68.4 | -47.6 | 47.7 | -126.2 | -55.5 | 58.5 | -13.8 | 2.8 | 0.0 |

$^1$excimer type, $^2$charge transfer type

Charge transfer (CT) excited states between donor (D) and acceptor (A) organic molecules along with metal-to-ligand charge transfer (MLCT) transitions in an iridium (III) dye are the last test cases investigated herein. In this context, DORI is complementary to other indexes, which serve to measure the spatial extent of charge transfer within molecules.[77–83] We first consider complexes formed by an aromatic donor (benzene, naphthalene and anthracene) and the tetracyanoethylene (TCNE) acceptor. For these complexes, the density-based descriptor naturally provides an intermolecular zone that can serve to identify charge transfer excitations. This intermolecular DORI clashing region shifts toward the charge depleted donor upon the formation of the $[D^+\text{-}A^-]^*$ excited complex. This is consistent with the fact that the acceptor's density expands after excitation as it carries more electrons. A similar pattern is obtained for ionic bonds (see e.g. LiF in Figure 7) and ground state charge transfer complexes. Taking the benzene-TCNE complex as an illustration, Figure 7 shows that the overlap of the two molecular density tails, and consequently the DORI clashing region, is shifted towards the donor in the $\pi\text{-}\pi^*$ charge transfer excited states ($S_1$) (see electron density difference in Figure 8 and Figure S8-10 for the molecular orbital pictures). This qualitative picture is nicely complemented by the integration of the electron density within the three DORI domains (Table 1). For the three considered charge transfer complexes, the trend is highly systematic and insightful: overall all the charge transfer excited states coincide with a decrease/increase in the number of electron within the donor/acceptor (A/B) in comparison with the ground state. Concurrently, the "I": integral goes down, thus reflecting the fact that the domain moves towards the electron donor, which has lost electron density. In a sense, this clash now reveals a concrete loss of electronic charge near the donor. Amongst the nine excited states investigated in Table 1, only the $S_3$ of the benzene-TCNE and anthracene-TCNE complexes correspond to a local excitation. These excitations, located on the TCNE and anthracene respectively (see electron density picture), are well captured by the DORI integrals that show a significant variation on the domain where the local excitation occurs but no change in the other molecular moiety or in the intermolecular domain. A somewhat weaker charge transfer character of $S_1$ in anthracene-TCNE is also detected both by the $DORI_{int}$ and the electron density difference.

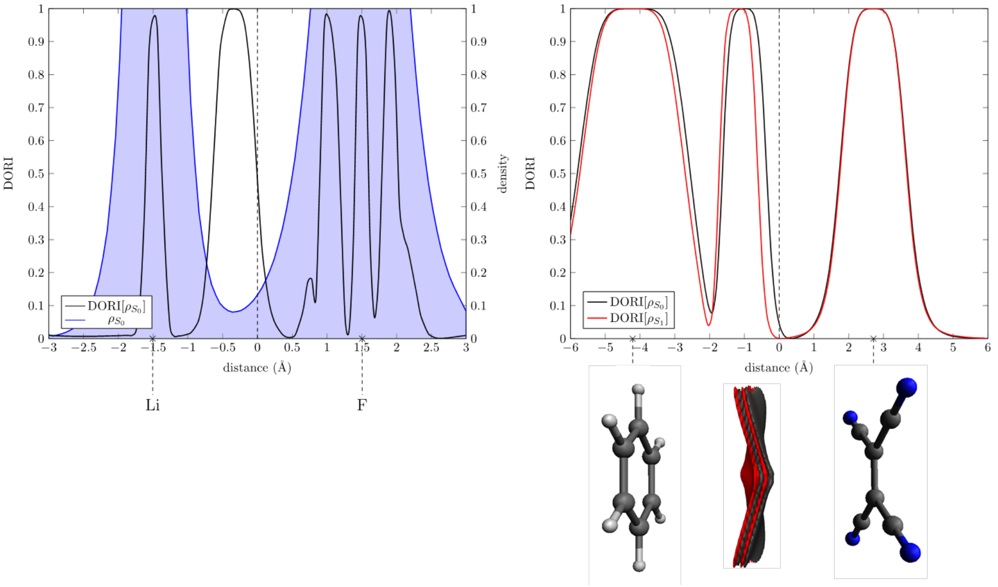

**Figure 7.** One-dimensional ground state (ground and excited states) DORI maps for the ionic LiF (left) and charge-transfer benzene-TCNE complex (right) plotted along the $C_n$ axis of the system. Relaxed densities to compute DORI are obtained at the (TD-)CAM-B3LYP/cc-pVDZ level (Bottom): Superposition of DORI[$\boldsymbol{\rho}$] = 0.9 in $S_1$ excited state (blue) and ground state (white) for the tetracyanoethylene - benzene dimer at the (TD-)CAM-B3LYP/cc-pVDZ level. The charge transfer is shown to induce a displacement of the DORI intermolecular basin towards the donor molecule.

Similar analyses enable the identification of $^1$MLCT excitations, such as those relevant to typical cyclometalated iridium (III) dyes. In the representative case visible in Figure 9, the $^1$MLCT nature of the first allowed transition (3.6 eV, f=0.1) can be identified by considering the metal (M) and ligands (L)-centered DORI integrals. The DORI integrals on the metal domain decrease upon excitation to $S_1$, while the one on the pyridine-containing ligand increases significantly. In contrast, the character associated with the phosphorescence from the (optimized) T1 states is essentially of ligand-centered character (see *e.g.* Ref. [84]) with no significant change in the DORI integrals associated with the iridium atom. This

This is the peer reviewed version of the following article: [*Chem. - Eur. J.* **2016**, *22*, 18442], which has been published in final form at https://chemistry-europe.onlinelibrary.wiley.com/doi/full/10.1002/chem.201603914. This article may be used for non-commercial purposes in accordance with Wiley Terms and Conditions for Use of Self-Archived Versions.

interpretation can indeed be validated by the electron density difference (Figure 9, bottom) and by the molecular orbital pictures (see supplementary information).

Overall, it is very appealing to see that the consideration of the three DORI integrals can be used to distinguish between different excited state characters without relying upon the orbital picture.

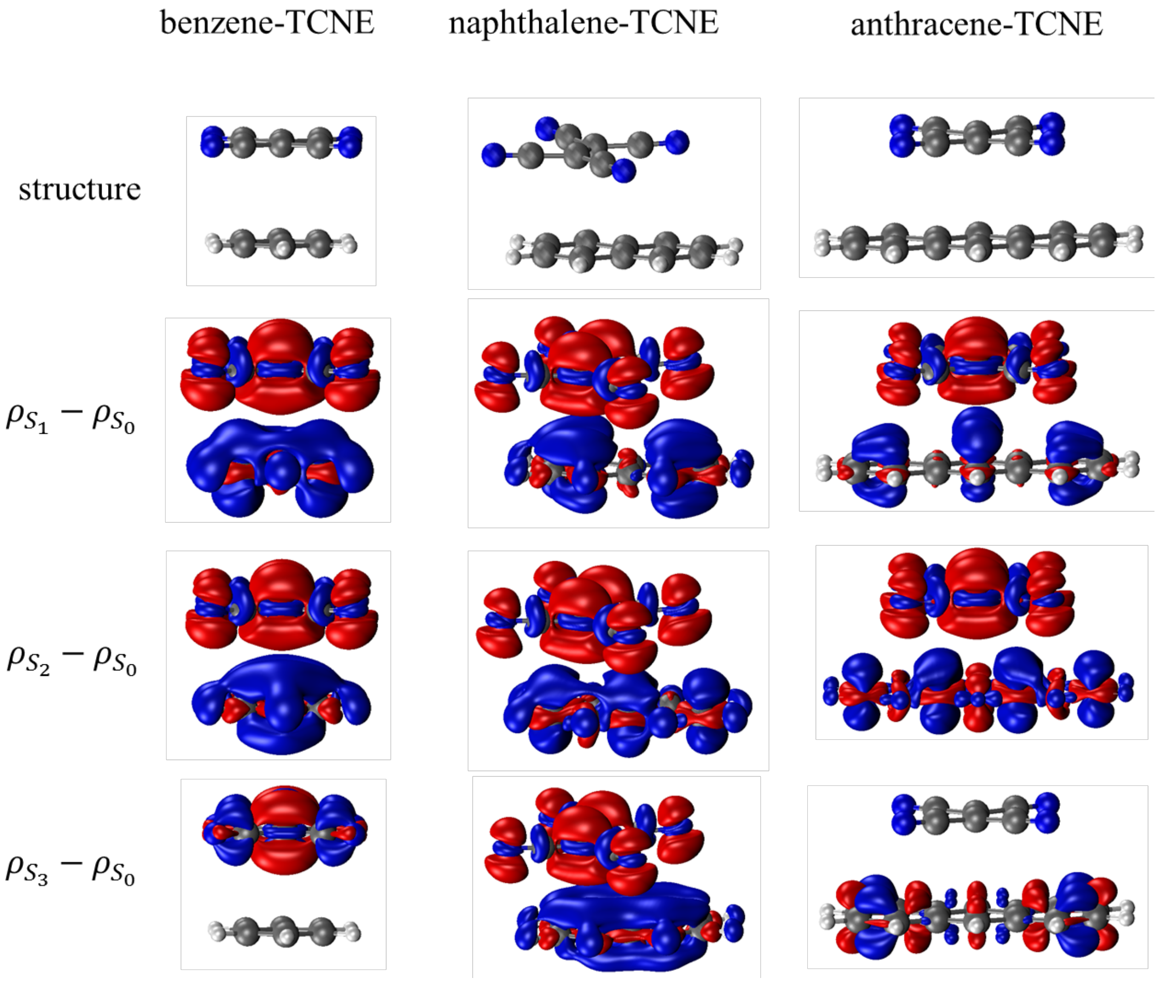

**Figure 8**: Density differences ($\rho_{S_n} - \rho_{S_0}$ , n∈{1, 2, 3}) at the (the (TD-)CAM-B3LYP/cc-pVDZ level for (top) benzene – TCNE (Isovalue □□±0.005), (middle) naphthalene-TCNE (Isovalue □□±0.005) and (bottom) anthracene-TCNE (Isovalue □□±0.0015). Positive values in red, negative in blue.

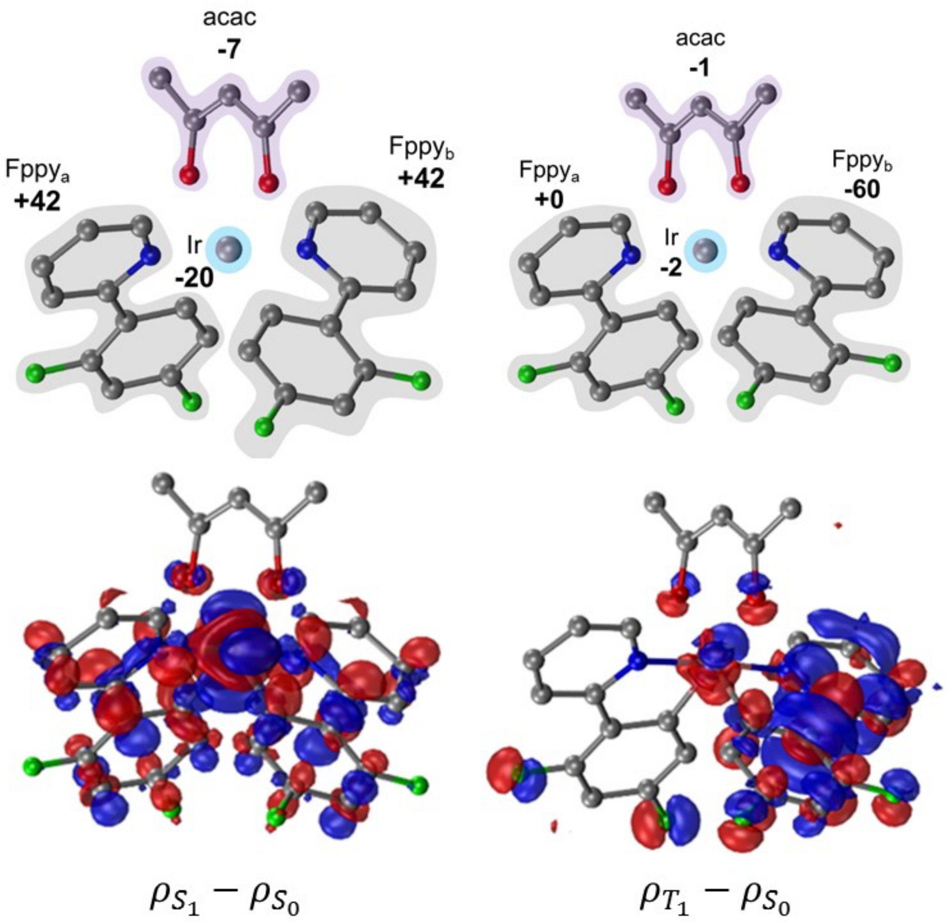

**Figure 9** (top) $\Delta\mathrm{DORI}_{\mathrm{int}} = [\mathrm{DORI}_{\mathrm{int}}(\boldsymbol{\rho}_{X_1}; V_{0.85}) - \mathrm{DORI}_{\mathrm{int}}(\boldsymbol{\rho}_{S_0}; V_{0.85})]*1000$ in milielectron (X=S,T) in the schematic DORI regions for Iridium (Ir), acetylacetonate (acac) and 2-(2,4-difluorophenyl)pyrydine (Fppy$_{a,b}$). (bottom) Density differences for the first singlet and optimized triplet excited states; isodensities=+0.002(red) and -0.002(blue). The scalar fields computed for absorption (left, $S_0 \rightarrow S_1$ in $S_0$ geometry) and emission (right, $T_1 \rightarrow S_0$ in the $T_1$ geometry) using the relaxed (TD-)CAM-B3LYP/cc-pVDZ densities. The complexes were optimized in the ground-state and first triplet at the (TD-)ωB97X-D/def2-SVP level.

## CONCLUSIONS

The first application of DORI to excited state situations is appealing. It allows an intuitive representation of the electronic and geometric modification occurring after electronic excitation processes in organic molecules solely based on their electronic density and its derivatives. The character of single molecule excitations is easily identifiable. Similarly, excimer formation can clearly be captured through a visual fingerprint derived from DORI scalar fields, bringing insights into the stacking behavior of these complexes. The impact of the intra- or intermolecular excited state processes on the density can also be analyzed through the integration of the (inter)molecular DORI basin, which is altered upon excitation. A net electron loss or gain is observed in the DORI basins characteristics of the transition, providing a straightforward tool for excited state complexes analysis.

## ACKNOWLEDGMENTS

The Swiss NSF Grant 156001 and EPFL are gratefully acknowledged for their funding support**.**

## Supporting Information

More details on the excitation energies, oscillator strengths, orbital contributions, DORI maps and geometries for the investigated single molecules and complexes.

## REFERENCES

[1] A. D. Becke, K. E. Edgecombe, *J. Chem. Phys.* **1990**, *92*, 5397.
[2] B. Silvi, A. Savin, *Nature* **1994**, *371*, 683–686.
[3] H. L. Schmider, A. D. Becke, *J. Mol. Struct. THEOCHEM* **2000**, *527*, 51–61.
[4] M. Kohout, *Int. J. Quantum Chem.* **2004**, *97*, 651–658.
[5] I. Fourré, B. Silvi, P. Chaquin, A. Sevin, *J. Comput. Chem.* **1999**, *20*, 897–910.
[6] H. Chevreau, I. de P. R. Moreira, B. Silvi, F. Illas, *J. Phys. Chem. A* **2001**, *105*, 3570–3577.
[7] S. Villaume, H. A. Fogarty, H. Ottosson, *ChemPhysChem* **2008**, *9*, 257–264.
[8] C. Dahlstrand, M. Rosenberg, K. Kilså, H. Ottosson, *J. Phys. Chem. A* **2012**, *116*, 5008–5017.
[9] J. Jara-Cortés, T. Rocha-Rinza, J. Hernández-Trujillo, *Comput. Theor. Chem.* **2015**, *1053*, 220–228.
[10] J. Contreras-García, E. R. Johnson, S. Keinan, R. Chaudret, J.-P. Piquemal, D. N. Beratan, W. Yang, *J. Chem. Theory Comput.* **2011**, *7*, 625–632.
[11] P. Popelier, *Coord. Chem. Rev.* **2000**, *197*, 169–189.
[12] R. F. W. Bader, *Atoms in Molecules: A Quantum Theory*, **1990**.
[13] H. Schmider, *J. Chem. Phys.* **1996**, *105*, 11134.

[14] Y.-G. Wang, K. B. Wiberg, N. H. Werstiuk, *J. Phys. Chem. A* **2007**, *111*, 3592–601.

[15] D. Ferro-Costas, A. M. Pendás, L. González, R. A. Mosquera, *Phys. Chem. Chem. Phys.* **2014**, *16*, 9249–58.

[16] V. Tognetti, L. Joubert, *Theor. Chem. Acc.* **2016**, *135*, 124.

[17] E. S. Kadantsev, H. L. Schmider, *Int. J. Quantum Chem.* **2008**, *108*, 1–14.

[18] T. Burnus, M. Marques, E. Gross, *Phys. Rev. A* **2005**, *71*, 010501.

[19] J. Cullen, M. Krykunov, T. Ziegler, *Chem. Phys.* **2011**, *391*, 11–18.

[20] T. Ziegler, M. Krykunov, J. Cullen, *J. Chem. Phys.* **2012**, *136*, 124107.

[21] H. J. Bohórquez, C. F. Matta, R. J. Boyd, *Int. J. Quantum Chem.* **2010**, *110*, 2418–2425.

[22] E. R. Johnson, S. Keinan, P. Mori-Sánchez, J. Contreras-García, A. J. Cohen, W. Yang, *J. Am. Chem. Soc.* **2010**, *132*, 6498–6506.

[23] P. de Silva, J. Korchowiec, T. A. Wesolowski, *ChemPhysChem* **2012**, *13*, 3462–3465.

[24] P. de Silva, J. Korchowiec, T. A. Wesolowski, *J. Chem. Phys.* **2014**, *140*, 164301.

[25] P. de Silva, J. Korchowiec, N. Ram J. S., T. A. Wesolowski, *Chim. Int. J. Chem.* **2013**, *67*, 253–256.

[26] P. de Silva, C. Corminboeuf, *J. Chem. Theory Comput.* **2014**, *10*, 3745–3756.

[27] E. J. Baerends, O. V. Gritsenko, R. van Meer, *Phys. Chem. Chem. Phys.* **2013**, *15*, 16408.

[28] A. V. Luzanov, A. A. Sukhorukov, V. E. Umanskii, *Theor. Exp. Chem.* **1976**, *10*, 354–361.

[29] R. L. Martin, *J. Chem. Phys.* **2003**, *118*, 4775.

[30] I. Mayer, *Chem. Phys. Lett.* **2007**, *437*, 284–286.

[31] M. Head-Gordon, A. M. Grana, D. Maurice, C. A. White, *J. Phys. Chem.* **1995**, *99*, 14261–14270.

[32] F. Plasser, M. Wormit, A. Dreuw, *J. Chem. Phys.* **2014**, *141*, 024106.

[33] F. Plasser, S. A. Bäppler, M. Wormit, A. Dreuw, *J. Chem. Phys.* **2014**, *141*, 024107.

[34] A. V Luzanov, *Russ. Chem. Rev.* **1980**, *49*, 1033–1048.

[35] A. V. Luzanov, O. A. Zhikol, *Int. J. Quantum Chem.* **2009**, NA–NA.

[36] V. Tognetti, C. Morell, P. W. Ayers, L. Joubert, H. Chermette, *Phys. Chem. Chem. Phys.* **2013**, *15*, 14465.

[37] R. A. Cormanich, M. Bühl, R. Rittner, *Org. Biomol. Chem.* **2015**, *13*, 9206–9213.

[38] S. Mebs, *Chem. Phys. Lett.* **2016**, *651*, 172–177.

[39] P. de Silva, C. Corminboeuf, *J. Chem. Phys.* **2015**, *142*, 074112.

[40] P. de Silva, C. Corminboeuf, *J. Chem. Phys.* **2015**, *143*, 111105.

[41] A. D. Becke, *J. Chem. Phys.* **1993**, *98*, 5648.

[42] M. Rosenberg, C. Dahlstrand, K. Kilså, H. Ottosson, *Chem. Rev.* **2014**, *114*, 5379–5425.

[43] E. Runge, E. K. U. Gross, *Phys. Rev. Lett.* **1984**, *52*, 997–1000.

[44] J.-D. Chai, M. Head-Gordon, *Phys. Chem. Chem. Phys.* **2008**, *10*, 6615–20.

[45] F. Weigend, R. Ahlrichs, *Phys. Chem. Chem. Phys.* **2005**, *7*, 3297–305.

[46] Gaussian 09, Revision **D.01**, M. J. Frisch, G. W. Trucks, H. B. Schlegel, G. E. Scuseria, M. A. Robb, J. R. Cheeseman, G. Scalmani, V. Barone, B. Mennucci, G. A. Petersson, H. Nakatsuji, M. Caricato, X. Li, H. P. Hratchian, A. F. Izmaylov, J. Bloino, G. Zheng, J. L. Sonnenberg, M. Hada, M. Ehara, K. Toyota, R. Fukuda, J. Hasegawa, M. Ishida, T. Nakajima, Y. Honda, O. Kitao, H. Nakai, T. Vreven, J. A. Montgomery, Jr., J. E. Peralta, F. Ogliaro, M. Bearpark, J. J. Heyd, E. Brothers, K. N. Kudin, V. N. Staroverov, R. Kobayashi, J. Normand, K. Raghavachari, A. Rendell, J. C. Burant, S. S. Iyengar, J. Tomasi, M. Cossi, N. Rega, J. M. Millam, M. Klene, J. E. Knox, J. B. Cross, V. Bakken, C. Adamo, J. Jaramillo, R. Gomperts, R. E. Stratmann, O. Yazyev, A. J. Austin, R. Cammi, C. Pomelli, J. W. Ochterski, R. L. Martin, K. Morokuma, V. G. Zakrzewski, G. A. Voth, P. Salvador, J. J. Dannenberg, S. Dapprich, A. D. Daniels, Ö. Farkas, J. B. Foresman, J. V. Ortiz, J. Cioslowski, and D. J. Fox, Gaussian, Inc., Wallingford CT, **2009**

[47] G. te Velde, F. M. Bickelhaupt, E. J. Baerends, C. Fonseca Guerra, S. J. A. van Gisbergen, J. G. Snijders, T. Ziegler, *J. Comput. Chem.* **2001**, *22*, 931–967.

[48] C. Fonseca Guerra, J. G. Snijders, G. te Velde, E. J. Baerends, *Theor. Chem. Accounts Theory, Comput. Model. (Theoretica Chim. Acta)* **1998**, *99*, 391–403.

[49] ADF2013, SCM, Theoretical Chemistry, Vrije Universiteit, Amsterdam, The Netherlands, Http://www.scm.com, P. M. E.J. Baerends, T. Ziegler, J. Autschbach, D. Bashford, A. Bérces, F.M. Bickelhaupt, C. Bo, T. H. Boerrigter, L. Cavallo, D.P. Chong, L. Deng, R.M. Dickson, D.E. Ellis, M. van Faassen, L. Fan, A. W. G. Fischer, C. Fonseca Guerra, M. Franchini, A. Ghysels, A. Giammona, S.J.A. van Gisbergen, H. J.A. Groeneveld, O.V. Gritsenko, M. Grüning, S. Gusarov, F.E. Harris, P. van den Hoek, C.R. Jacob, E. van Jacobsen, L. Jensen, J.W. Kaminski, G. van Kessel, F. Kootstra, A. Kovalenko, M.V. Krykunov, L. Lenthe, D.A. McCormack, A. Michalak, M. Mitoraj, S.M. Morton, J. Neugebauer, V.P. Nicu, W. Noodleman, V.P. Osinga, S. Patchkovskii, M. Pavanello, P.H.T. Philipsen, D. Post, C.C. Pye, J. G. Ravenek, J.I. Rodríguez, P. Ros, P.R.T. Schipper, G. Schreckenbach, J.S. Seldenthuis, M. Seth, O. V. Snijders, M. Solà, M. Swart, D. Swerhone, G. te Velde, P. Vernooijs, L. Versluis, L. Visscher, A. L. Y. F. Wang, T.A. Wesolowski, E.M. van Wezenbeek, G. Wiesenekker, S.K. Wolff, T.K. Woo

[50] E. Van Lenthe, E. J. Baerends, *J. Comput. Chem.* **2003**, *24*, 1142–56.

[51] K. B. Wiberg, C. M. Hadad, T. J. LePage, C. M. Breneman, M. J. Frisch, *J. Phys. Chem.* **1992**, *96*, 671–679.

[52] N. C. Handy, H. F. Schaefer, *J. Chem. Phys.* **1984**, *81*, 5031.

[53] M. Kohout, *DGRID, Version 4.6, Radebeul*, **2011**.

[54] C. Henderson, A.; Ahrens, J.; Law, *The ParaView Guide ; Kitware Clifton Park, NY*, **2004**.

[55] *ADF2016, SCM, Theoretical Chemistry, Vrije Universiteit, Amsterdam, The Netherlands, Http://www.scm.com.*

[56] B. O. Roos, P.-Åke Malmqvist, V. Molina, L. Serrano-Andrés, M. Merchán, *J. Chem. Phys.* **2002**, *116*, 7526.

[57] X. Li, J. Paldus, *J. Phys. Chem. A* **2010**, *114*, 8591–8600.

[58] O. Christiansen, J. Gauss, J. F. Stanton, P. Jo/rgensen, *J. Chem. Phys.* **1999**, *111*, 525.

[59] M. Barbatti, J. Pittner, M. Pederzoli, U. Werner, R. Mitrić, V. Bonačić-Koutecký, H. Lischka,

*Chem. Phys.* **2010**, *375*, 26–34.

[60] C. Adamo, V. Barone, *J. Chem. Phys.* **1999**, *110*, 6158.

[61] N. C. Baird, *J. Am. Chem. Soc.* **1972**, *94*, 4941–4948.

[62] A. Samanta, C. Devadoss, R. W. Fessenden, *Chem. Phys. Lett.* **1990**, *169*, 421–426.

[63] Z. B. Maksic, D. Kovacek, M. Eckert-Maksic, M. Bockmann, M. Klessinger, *J. Phys. Chem.* **1995**, *99*, 6410–6416.

[64] A. Stanger, *J. Am. Chem. Soc.* **1991**, *113*, 8277–8280.

[65] E. Steiner, P. W. Fowler, *Int. J. Quantum Chem.* **1996**, *60*, 609–616.

[66] S. N. Steinmann, D. F. Jana, J. I.-C. Wu, P. von R. Schleyer, Y. Mo, C. Corminboeuf, *Angew. Chem. Int. Ed. Engl.* **2009**, *48*, 9828–33.

[67] F. M. Winnik, *Chem. Rev.* **1993**, *93*, 587–614.

[68] J. B. Birks, *Photophysics of Aromatic Molecules*, Wiley, London, **1970**.

[69] M. Parac, S. Grimme, *Chem. Phys.* **2003**, *292*, 11–21.

[70] J. C. Amicangelo, *J. Phys. Chem. A* **2005**, *109*, 9174–82.

[71] T. Rocha-Rinza, L. De Vico, V. Veryazov, B. O. Roos, *Chem. Phys. Lett.* **2006**, *426*, 268–272.

[72] R. Huenerbein, S. Grimme, *Chem. Phys.* **2008**, *343*, 362–371.

[73] T. Rocha-Rinza, O. Christiansen, *Chem. Phys. Lett.* **2009**, *482*, 44–49.

[74] S. Shirai, S. Iwata, T. Tani, S. Inagaki, *J. Phys. Chem. A* **2011**, *115*, 7687–99.

[75] K. Diri, A. I. Krylov, *J. Phys. Chem. A* **2012**, *116*, 653–62.

[76] M. Kołaski, C. R. Arunkumar, K. S. Kim, *J. Chem. Theory Comput.* **2013**, *9*, 847–856.

[77] M. J. G. Peach, P. Benfield, T. Helgaker, D. J. Tozer, *J. Chem. Phys.* **2008**, *128*, 044118.

[78] T. Le Bahers, C. Adamo, I. Ciofini, *J. Chem. Theory Comput.* **2011**, *7*, 2498–2506.

[79] C. A. Guido, P. Cortona, B. Mennucci, C. Adamo, *J. Chem. Theory Comput.* **2013**, *9*, 3118–3126.

[80] C. A. Guido, P. Cortona, C. Adamo, *J. Chem. Phys.* **2014**, *140*, 104101.

[81] T. Etienne, X. Assfeld, A. Monari, *J. Chem. Theory Comput.* **2014**, *10*, 3896–3905.

[82] T. Etienne, X. Assfeld, A. Monari, *J. Chem. Theory Comput.* **2014**, *10*, 3906–3914.

[83] C. Adamo, T. Le Bahers, M. Savarese, L. Wilbraham, G. García, R. Fukuda, M. Ehara, N. Rega, I. Ciofini, *Coord. Chem. Rev.* **2015**, *304-305*, 166–178.

[84] J. Frey, B. F. E. Curchod, R. Scopelliti, I. Tavernelli, U. Rothlisberger, M. K. Nazeeruddin, E. Baranoff, *Dalt. Trans.* **2014**, *43*, 5667–5679.

Graphical Abstract:

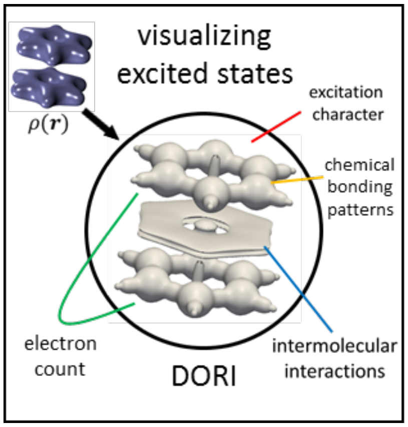

**Scrutinizing excited states:** The nature of chemical bonding in the excited state remains relatively unexplored. The Density Overlap Region Indicator (DORI) is ideally suited for this purpose. We here demonstrate its usefulness through visual and numerical DORI signatures for both intra- and intermolecular excited state situations.

Keywords: bonding descriptor, excited states, DORI